2012 Intelligent Vehicles Symposium
Alcalá de Henares, Spain, June 3-7, 2012

Robust Extraction of Lane Markings Using Gradient Angle Histograms and Directional Signed Edges

R. K. Satzoda, S. Suchitra and T. Srikanthan

Abstract— **In this paper, we propose novel block-based techniques for robust extraction of lane marking edges in complex scenarios, such as in the presence of shadows, vehicles, other road markings etc. The techniques are based on the properties of lane markings and involve a two-stage processing: (1) generation of customized edge maps using histograms of gradient angles, and (2) directional signed edges in combination with Hough Transform to identify lane markings. It is shown that the proposed techniques show a detection accuracy of as high as 98% on test data collected on real road scenarios, representing the various complex cases.**

I. Introduction

Lane detection is a crucial task in many ADAS (Advanced Driver Assistance Systems) applications, such as lane departure warning, lane change assistance etc [1]. Almost all existing approaches to lane detection involve lane feature extraction as the core step, the output of which is fed into post-processing steps. Depending on the end application and method employed, the postprocessing steps range from use of computational models such as curves, splines etc., to neural networks to template matching to RANSAC to Hough Transform [1], [2]. A detailed survey of these vision based lane detection techniques are discussed in [1], [2]. Given the complex road scenarios with varying lighting conditions, shadows, vehicles and other features on the road, robust lane extraction is often a challenge [2]. We briefly discuss some related work below before proposing our contribution in this area.

A. Existing work on Lane Feature Extraction

Although many approaches have been proposed to extract lane markings in complex scenarios, this problem continues to be researched upon. Various kinds of techniques involving gradient magnitudes, edge density functions (EDF), Gabor filters, Hough transform etc. are used to extract lane features. Lindner et al. [3] use features that are extracted at multiple levels for geometric lane feature extraction. Gradient magnitude values are used to construct line segments, parallel lines, curves and then detect lane markings. Coskun et al. [4] use warp perspective mapping (WPM) to get a top view and then apply Gabor filters to narrow down lane markings. Zhou et al. [5] employ Gabor filters on image intensities to initially determine the vanishing point, followed by Canny edge detector along with Hough Transform to detect lane edges in the near view. Lee et al. [6] proposed a lane extraction method that uses an Edge Density Function (EDF) recursively over a set of frames to offset noise effects, where noise is defined as any feature that is misdetected as lane marking. Tsai et al. [7] consider lane markings as high contrast color features against the road and employ morphology in conjunction with modeling like straight line fitting model and Markov modeling. Otsuka et al. [8] use local edge direction using zero crossings for detecting straight lane markers and raised pavement markers.

However, the success of many of the above methods, largely depends on the effectiveness of the edge detector. For example, in [3], the quality of lane extraction greatly depends on the results of the Canny edge detection and hence not always consistent. This is the case in [6] also. Moreover, many of the above recent work do not address the issue of shadows and other features that tend to yield false positives. For example, in [4], shadows and other obstructions can be falsely picked up by Gabor filters. Similarly, in the method in [6], the EDF does not give accurate results in the presence of shadows and other edges with the same angles as lanes, such as pavements. Also, since EDF is generated over large blocks of image in a global manner, noise from shadows, vehicle edges etc. can affect the detection of peaks (which represent lane markings) in the EDF. In [8], in order to capture lane markings with very low contrast, threshold for edge detection is reduced. This will however, add more edge content from shadows of trees, vehicles etc. Moreover, checking edge direction of pixels is performed as a local operation, as a result of which, stray outliers from shadows and other features having the same direction towards the vanishing point, are also picked up.

To summarize, robust extraction of lane marking edges in complex road scenes is still a challenging problem. Also, as seen in the above references, effectiveness of edge extraction of lane markings is crucial in various ADAS applications, as the edge map generated affects the subsequent processing steps. In this paper, we present a novel method to achieve robust lane edge feature extraction in complex scenarios such as presence of noise, shadows, vehicles etc. The proposed method uses simple histograms of gradient angles to generate what we call as directional signed edges. These directional signed edges are then analyzed in an informed manner using Hough Transform, such that only the lane markings are extracted and rest of the non-lane features are eliminated.

The rest of the paper is organised as follows. The next subsection (Section I-B) describes the different types of complex road scenarios we see during lane marking extraction. In Section I-C, we define the region of interest (RoI). In Section II, we describe the proposed method in detail. The overview of the proposed method is presented in Section II-A, followed by the different stages in the method in Section II-B and II-C. The results are presented and discussed in Section III before

978-1-4673-2118-1/$31.00 ©2012 IEEE

making concluding remarks in Section IV.

B. Complex Scenarios

In this section, we define what we mean by complex scenarios so that the context of the proposed work is clearly defined in the rest of the paper. What makes feature-based extraction of lane markings from highways, into a complex problem, is the presence of other features such as shadows, vehicles etc. in the road scene, which often tend to mix with the lane features, thereby causing misdetections. The various complex scenarios are grouped into three major categories, as listed below:

- Type A: This refers to "random" features such as shadows from trees; random because the boundaries of these shadows do not necessarily follow any geometrical property. This is one of the most common problems, wherein shadows from trees fall on the lane markings and create unwanted edge pixels, thereby making it difficult to differentiate edge pixels belonging to lane markings from those of shadows (Fig. 1(a)).
- Type B: This refers to geometrical features in the road scene, with linear boundaries. Having linear boundaries is a property of lane markings, but other features in the road scene, such as shadows from overhead bridges, lamp posts etc. also have linear edges, and fall in the region of lane markings, which can cause false positives. Example of a road scene with a shadow of an overhead bridge is shown in Fig. 1(b).
- Type C: This includes geometrical features that not only have linear boundaries, but are also aligned towards the vanishing point, just like lane markings. This refers to those features that bear a very close semblance to lane markings, hence increasing the chances of mistaking such features for road markings. Examples of this are pavements, edges of long vehicles on side lanes, other road markings on the lane such as arrows etc (Fig. 1(c)). Sometimes, some lanes or parts of a lane are in a different road tar color from the rest, which can also result in linear edges aligned towards the vanishing point (Fig. 1(d)).

We propose efficient techniques that extract lane markings which are found amidst all the above three types of complex road scenarios.

C. Region of Interest (RoI)

It has been proposed in [6] to divide the road scene into two horizontal slices - near view and far view, for the sake of processing the image more meaningfully to extract lane markings. Near view, which represents the bottom slice of image, captures the immediate patch of road surface in front of the host vehicle and far view refers to the road scene further away from the vehicle. It has also been shown [6], [8] that lane markings in the near view are more predictable in terms of their positions and angle, with respect to the host vehicle. Even in the case of curved lanes, the curvature is more visible in the far view, and the lanes continue to appear as straight lines in the near view, thus making it more predictable to process. What is important to note is that near view lane markings can be used to detect the far view curvature of the lane markings. For example, linear approximation has been employed in [3] to detect curved lanes by first detecting linear segments in the near view. Similarly in [5], near view results of lane detection are used to infer the far view lanes via tracing algorithms.

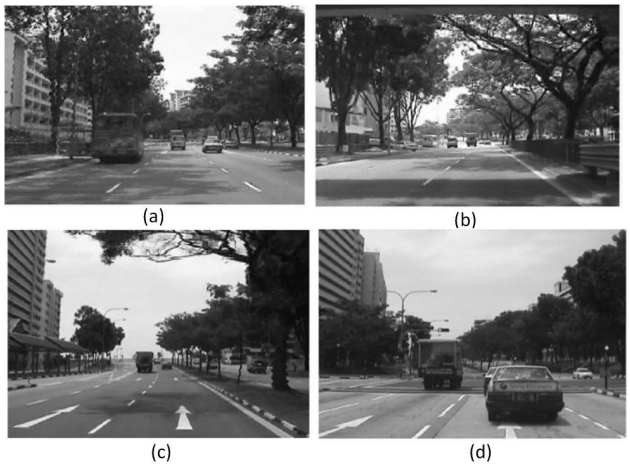

Fig. 1. Complex road scenes making lane extraction a challenging problem (a) Type A: Shadows of trees fall on the road surface creating random features, (b) Type B: Dark shadow of the over head bridge creates linear edges; other examples include lamp posts etc., (c) & (d) Type C: Linear edges that are in the direction of the vanishing point - arrow markings (c) and road tar color change (d)

Considering that accurate detection of lane markings in the *near* view is crucial, we will be focussing on the lane markings in the near view only, in this paper. However, all the steps proposed in the method can be applied to lanes in far view also, with some additional processing.

II. Proposed Method

A. Overview of the Proposed Method

The rationale behind the proposed method for lane features extraction from complex road scenarios, is to closely align each step of the method with the properties of lane markings. We make use of the distinct properties of the lane markings, especially in the near lanes, to distinguish them from shadows, overhead fixtures, railings etc. We list the distinct properties of lane markings, P1 to P4, as follows:

- *P1*: The pixels forming the edge of the lane markings have similar gradient angles. This is because the lane markings in the RoI are linear.
- *P2*: The lane markings occur at predictable locations with respect to the host vehicle. They point towards the vanishing point, hence also having predictable angle of orientation.
- *P3*: Each lane marking is bound by a pair of linear edges of opposite nature - left edge, where the intensity transition is from the dark road surface to the relatively light colored lane marking, and right edge, where the intensity transitions from the light lane marking intensity back to dark road surface.

- *P4*: The distance between left and right edges in the lane marking, is a known priori. This is a safe assumption because in the near view, the width of the lane markings is a fixed known value and does not change. We call this 'thickness criteria'.

The proposed method employs simple computational steps for extracting lane marking features by exploiting the above properties of lane markings $P1$ to $P4$. The proposed method is broadly divided into two stages, where the first stage is based on $P1$ and $P2$, and second stage is based on $P3$ and $P4$. The steps, as shown in Fig. 2, are outlined below:

- *Stage 1*: In this stage, we propose the use of histograms of gradient angles (called GAH) in a block-based fashion to generate a customized edge map (called 'Straight Line Edge Map' or $SLEM$). The resulting edge map from this stage comprises of straight line edges only and are pointed in the direction of the lane towards the vanishing point. The output of this stage is sent to Stage 2.
- *Stage 2*: This stage performs the final filtering of the lane candidates sent from Stage 1. We propose directional edge generation and detection to confirm/reject the lane candidate edges sent from Stage 1.

More details on the above two steps are discussed in the following sections.

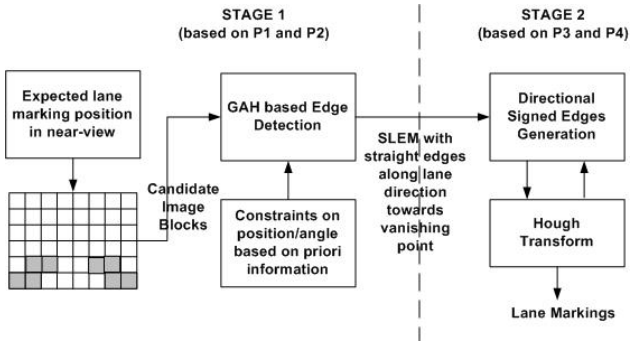

Fig. 2. Basic Processing Steps in the Proposed Method

B. Stage 1: Customized edge map generation using GAH and RoI blocks

This stage makes use of lane properties $P1$ and $P2$ to filter the possible lane marking candidates. $P1$ is used to selectively construct an edge map that contains only straight lines, and rejecting non-linear features. $P2$, which gives priori information on expected position and angle of the lane markings, is used for both extracting the region of interest, and eliminating many of the non-lane linear features.

The first step in Stage 1 is to select the region of interest (RoI), the region in the image where lane markings are expected. As indicated earlier, processing is performed on the near view of the road surface, which is divided into blocks. The lower 1/4-th of the image is taken as the near region of interest, which is divided into equal blocks. The advantage of using block-based processing is that it allows sensitivity

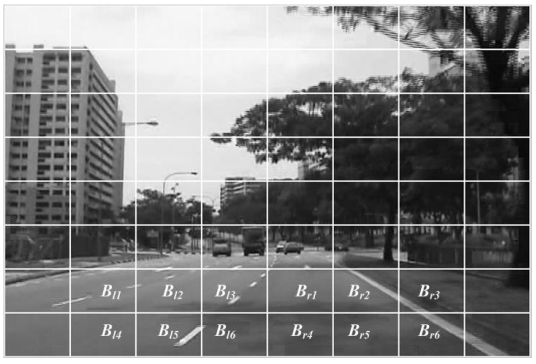

Fig. 3. Image is divided in blocks. The near view RoI comprises of the blocks in the last two rows. Based on Property $P2$ the blocks B_{l1} to B_{l6} are selected for left lane detection and B_{r1} to B_{r6} are selected for right lane detection

to local changes within the image. Moreover, it also allows a more controlled analysis of the histograms, which we will be generating in this stage. Property $P2$ is used to select the blocks of interest in the RoI. We know that a right-slanting lane marking appears in the left half of the near-view and a left-slanting lane marking appears in the right half of the near view. The width of the lane and the expected position of the lane markings are also predictable. Based on this, the candidate blocks are selected in the lowest rows of blocks, separately for left lane detection and right lane detection. Fig. 3 shows the different blocks selected in the RoI for left and right lane processing in the near view based on $P2$.

Once the blocks are selected, the next step is to construct a gradient map for these blocks. For an image block B_i, the horizontal and vertical Sobel kernels [9] are applied to get signed horizontal and vertical gradient values $\nabla_y B_i$ and $\nabla_x B_i$ respectively. These are used to compute the gradient magnitudes $|\nabla B_i|$ and angles $\nabla_\theta B_i$ of all the pixels in the block B_i using:

$$\begin{aligned} |\nabla B_i(x,y)| &= \sqrt{|\nabla_y B_i(x,y)|^2 + |\nabla_x B_i(x,y)|^2} \\ \nabla_\theta B_i(x,y) &= tan^{-1}\left(\nabla_y B_i(x,y)/\nabla_x B_i(x,y)\right) \end{aligned} \quad (1)$$

where (x,y) are the indices of a pixel in B_i.

The next step is based on $P1$. Our previous work in [10], uses gradient angle histograms (referred to as GAH) in a block-based manner, to generate edge maps containing only straight lines, referred to as 'Straight Line Edge Map' (SLEM). The GAH is used as an initial indicator for presence of straight lines in that block. This is because pixels along a straight line have similar gradient angles, and this manifests as a peak in the GAH. This step serves as an effective way to reduce computations in the Hough Transform step in Stage 2, and leads to cleaner Hough spaces [10] for robust analysis.

In order to do this, for each block B_i, we first compute an initial edge map by thresholding the gradient magnitudes $|\nabla B_i(x,y)|$ (this thresholding process is explained in [10]). We then compute the GAH for B_i, represented by GAH_{Bi}, which gives the distribution of gradient angles $\nabla_\theta B_i$s of all edge pixels in B_i. A peak in GAH_{Bi} at an angle θ_p indicates a possibility of a straight line edge along θ_p. Since

lane markings in the near view are straight lines, the edge pixels on them will group together as a peak in GAH.

Furthermore, we know the possible angle range, which defines the orientation of the lane markings in the near view ($P2$). So, we restrict the search for the peak in the GAH in pre-defined angle ranges given by $\Delta_L = [\theta_{Ll}, \theta_{Lu}]$ and $\Delta_R = [\theta_{Rl}, \theta_{Ru}]$, where Δ_L and Δ_R are the angle ranges for left and right lanes respectively. We select only those edge pixels from each block, which give a peak in the expected angle ranges in GAH. This will help to eliminate unwanted lines formed due to shadows and other features that are not aligned in the same direction as the lane. This eliminates noisy edges formed from Type A and B scenarios, discussed in Section I-B.

If a peak is detected at an angle θ_p in GAH_{Bi} such that θ_p is within Δ_L or Δ_R, the peak height n_{θ_p} gives the number of edge pixels having the gradient angle θ_p. We consider the edge pixels in the neighboring bins of GAH, i.e., $\theta_p \pm \delta$ to accommodate slight variations in the gradient angles of edge pixels along a line. If n_{θ_p} is greater than a minimum number of edge pixels, n_{th}, that is required to satisfy a straight line condition, we consider those edge pixels in the selected bins in GAH and create the straight line edge map E_{SL}. We then proceed to the next computational stage. If not, the next potential block in the region of interest is selected and its GAH is computed.

Fig. 4 shows the result of applying Stage 1 processing steps on an image block (Fig. 4(a)) with a right lane marking. Fig. 4(b) is the initial edge map formed by thresholding the gradient magnitudes. It can be seen that this edge block has both lane marking edges and some noise edge pixels that are not in the direction of the lanes. When the GAH is computed for these edge pixels, as shown in Fig. 4(c), two peaks are formed, one centering around $\theta_{p1} = 0^o$ and the second one at $\theta_{p2} = -20^o$. From the priori knowledge, it is known that the right lanes will occur in an angle range of $\Delta_R = [-40^o, -15^o]$. With this information at hand, the first peak centering at 0^o is rejected and the second peak is selected because $\theta_{p2} \in \Delta_R$. Fig. 4(d) plots the edge pixels that have a gradient angle which form the second peak in GAH at 35^o. The noisy edge pixels that are not a part lane edges are eliminated and the edge pixels that appear to be a part of lane markings only are picked up.

C. Stage 2: Directional Signed Edges Generation & Confirming Lane Markings

The edge pixels released from GAH are expected to be straight line edges. In order to verify whether these edge pixels are indeed the lane markings, we use the third property ($P3$) of lane markings, i.e., a lane marking has a left edge formed by dark to light transition, and a right edge formed by light to dark transition. To achieve this, we first spilt the edge pixels in straight line edge map E_{SL} into two groups using the equations below:

$$\begin{aligned} E_{SLl} &= \{E_{SLl}(x,y) : \nabla_x B_i(x,y) >= 0\} \\ E_{SLr} &= \{E_{SLr}(x,y) : \nabla_x B_i(x,y) < 0\} \end{aligned} \quad (2)$$

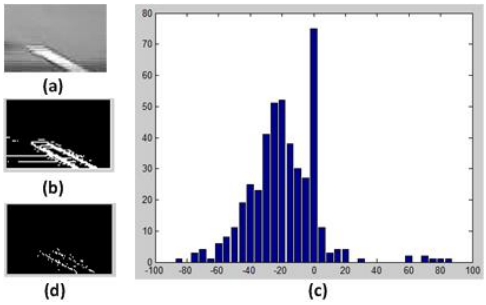

Fig. 4. (a) Image block with right lane marking and shadows, (b) Initial edge map with both lane marking edges and the shadow edges (noise), (c) Gradient angle histogram (GAH) for the input edge pixels of block, (d) Edge pixels E_{SL} of straight line edges corresponding to the peak centering -20^o.

where E_{SLl} has the edge pixels that show dark to light intensity transition, and the edge pixels in E_{SLr} show light to dark intensity transition. We call these edge maps *directional signed edge maps*. According to Properties $P3$ and $P4$ of a lane marking, we should get two straight line edges L_l and L_r, which transit from dark→light and light→dark respectively and are separated by a small distance $\Delta\rho_{lr}$. In other words, if E_{SL} does indeed have a lane marking, E_{SLl} and E_{SLr} capture the left edge and right edge of the lane marking respectively.

Given the two edge maps E_{SLl} and E_{SLr}, we now perform the final check to see if E_{SLl} and E_{SLr} have two parallel lines, one in each, that are separated by a small distance $\Delta\rho_{lr}$ ('thickness criteria' in $P4$). In order to do this, we compute Hough transform for E_{SLl} to give a Hough space HS_l. We check for any peaks in HS_l in the predefined angle range for the lanes. Let us say, we get a peak at (ρ_l, θ_l) in HS_l. We then compute the HT of E_{SLr} for a small angle range around θ_l resulting in Hough space HS_r. This is done because, the lanes edges in E_{SLl} and E_{SLr} are expected to be parallel edges, i.e., they must be having similar angles in Hough space. If we get a peak at (ρ_r, θ_r) in HS_r, then we proceed to find:

$$\Delta\rho = |\rho_l - \rho_r| \quad \Delta\theta = |\theta_l - \theta_r| \quad (3)$$

The straight line edges in E_{SLl} and E_{SLr} are confirmed as lane markings if,

$$(\Delta\theta < \Delta\theta_{lr}) \ AND \ (\Delta\rho < \Delta\rho_{lr}) \quad (4)$$

where $\Delta\theta_{lr}$ is a small angle range. $\Delta\theta < \Delta\theta_{lr}$ implies that the edges belong to parallel straight line edges. In addition, if $\Delta\rho < \Delta\rho_{lr}$ is also satisfied, then the straight line parallel edges, one in E_{SLl} and the other in E_{SLr}, are separated by a small distance. This satisfies the Properties $P3$ and $P4$ of lane markings.

This process is performed for all peak pairs, one from HS_l and the other from HS_r. If atleast one pair is found that satisfies all the above conditions, then we consider that image block to have a lane marking.

We illustrate the above mentioned process using the example shown in Fig. 5. The selected block shown in Fig.

5(a) gives the edge map E_{SL} shown in Fig. 5(b) after Stage 1 processing. It can be seen that Stage 1 processing has eliminated all edges except those straight line edges that are in the direction of the left lane. In Fig. 5(b), there are both valid lane marking boundaries and an edge that does not belong to a valid lane boundary, i.e., the edge formed by tar color change. When E_{SL} is split into the left and right directional edge maps E_{SLl} and E_{SLr}, we get the edges shown in Fig. 5(c) and (d). It can be seen that E_{SLl} has two edges corresponding to dark→light intensity transitions, one from the lane marking and other from the dark tar color to light tar color. However, E_{SLr} has one edge corresponding to the light→dark transition of the lane marking. We now have to identify which is the lane marking from these edges. On applying HT to E_{SLl} and E_{SLr}, we get the following (ρ, θ) tuples in their respective Hough spaces HS_l and HS_r: $(502, 40^o)$ and $(515, 49^o)$ in HS_l, and $(506, 43^o)$ in HS_r. Amongst these (ρ, θ) tuples, the pair - $(502, 40^o)$ in HS_l and $(506, 43^o)$ in HS_r satisfies the Δ_ρ and Δ_θ conditions in equation (3). Therefore the edges of the lane markings only are picked up and the other edge, made by tar color change in the direction of the lane, is rejected as shown in Fig. 5(e).

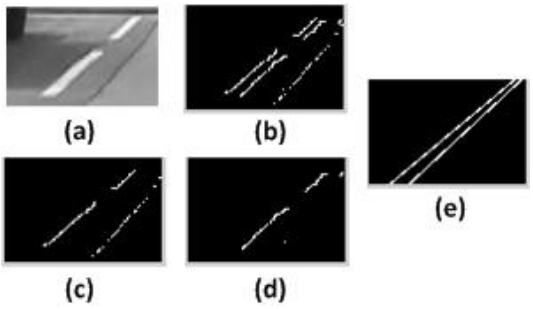

Fig. 5. Stage 2 processing illustration: (a) Image block with lane markings and other edges like tar color change along the direction of the lane (Type C scenario), (b) Straight line edge map E_{SL} obtained from Stage 1, (c) Left directional edge map E_{SLl} with the left lane marking edge and the tar color change edge also, (d) Right directional edge map E_{SLr} with the right lane marking edge, (e) Resulting straight lines that are identified as having the lane markings after analysing the Hough spaces

III. Results & Discussion

In this section, we present a discussion on the effectiveness of the proposed method to detect near lane markings in various scenarios. The test images are extracted from a video that was captured on Singapore highways and major roads over a stretch of 15 kilometers during day time and late evening time. Over 3400 image frames were used to test the effectiveness of the proposed method. These test images include the different types of complex road scenarios described in Section I-B. The proposed method showed nearly 98% accuracy in detecting the lane markings amidst various complex road scenarios in near view.

1) Valid Near Lane Marking Detection: Fig. 6 shows the near lanes identified by the proposed method in the different complex scenarios Types A, B and C. The proposed method is able to identify the near lane markings in the presence of randomly scattered shadows of trees, with and without vehicles (Fig. 6(a) & (b)), uniform shadows of overhead bridges (Fig. 6(c)), shadows of vehicles that are closely following the lane markings (Fig. 6(d)) and tar color changes (Fig. 6(e)). Each of these scenarios is discussed below.

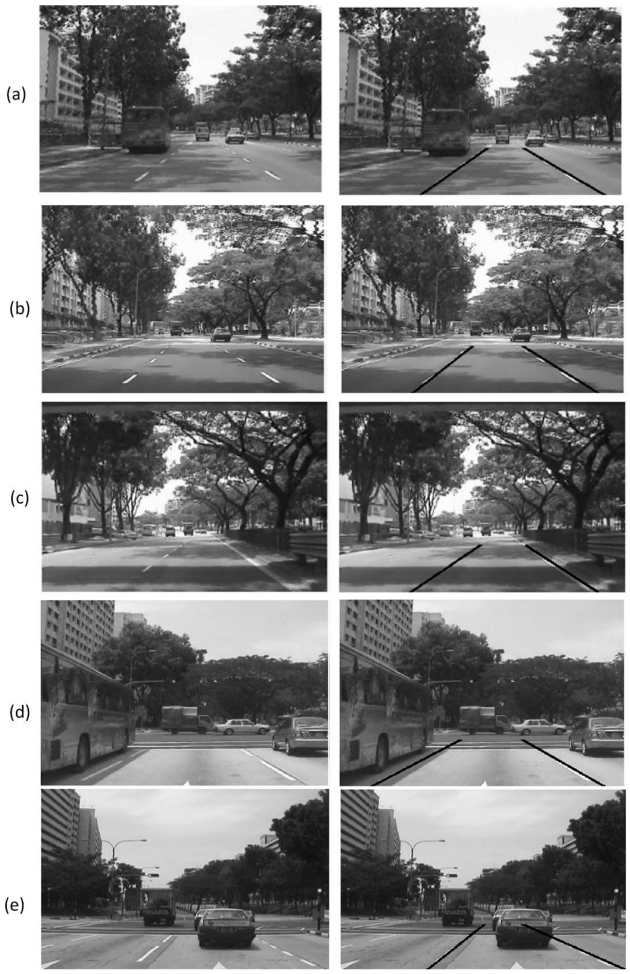

Fig. 6. Near lane detection in complex scenarios: Type A - shadows of trees and other random features (a) & (b), Type B - shadows of overhead bridges (c) etc. with straight line features not along lanes, Type C - Features like shadows of vehicles (d) and tar color change edges (e) in the direction of lanes

Shadows from trees do not necessarily conform to any property and are quite random in their distribution. As explained, the proposed method does not process a raw edge map, but works on a $SLEM$ constructed using GAH, that contains only straight line edges. This eliminates most of the edge pixels forming boundaries of tree shadows. Sometimes shadows from trees do give horizontal edges. Again, these are filtered out by setting the appropriate angle range in GAH and by checking for peaks only in those angle ranges. In the case of shadows from overhead bridges and other fixtures such as lamp posts, the edges are usually not along the lane. Setting the desired angle range in GAH can filter out line edges that are present at any other angular orientation, other than that of the lane markings.

Fig. 7. Lane marking detection using proposed method in the presence of edges that are along the direction of lanes towards the vanishing point: (a) & (b) show tar road color changes that create edges along the lanes, (c) shows the presence of vehicle shadows in the direction of lanes.

Edges from vehicles are usually linear and also aligned towards the vanishing point, just like lane markings. If these vehicle edges fall in the expected position of lane markings, then it normally leads to mis-detections. Similarly, features such as tar color of the road changing uniformly along the lane, leads to straight line edges in the direction/position of lane markings. It is more difficult to differentiate these features because they show similar properties as lane markings in terms of their orientation and position. However, the use of directional edges with Hough Transform and the thickness criteria in Stage 2 of the proposed method successfully eliminates these edges from being considered as lane markings. Some of these cases are shown in Fig. 7.

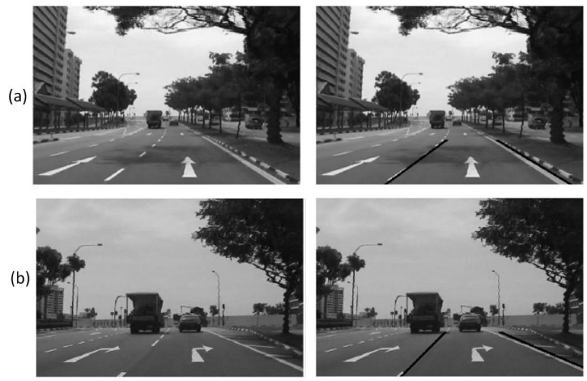

Fig. 8. Lane marking detection in the presence of other road markings

We also show the effectiveness of the proposed method in extracting lane markings in the presence of other road markings. Fig. 8 shows two of these cases. The different kinds of arrows in Fig. 8 are rejected and the lane markings only are detected in the near view. These different road markings are differentiated in the proposed method based on the fact that arrows and other road markings do not have parallel edges and usually fail the 'thickness criteria'.

2) Mis-detections: There was a small percentage of mis-detections (about 2%) in the whole set of over 3400 test cases. Some of the common mis-detections happen when the vehicle is changing lanes. When this happens, the positions/orientations of the lane markings, which is a priori information, is altered and hence leads to mis-detections. Other cases of mis-detections include when the lanes are smudged or when the lanes are faded to an extent that their edges do not form any straight line edges. When the lighting on the road surface was poor, e.g. during late evening time, the lanes were not correctly detected.

IV. Conclusion

In this paper, we described a novel two-stage method that detects the presence of lane markings effectively, in the presence of various non-lane marking features on the road surface. It was shown how the inherent properties of lane markings are exploited to selectively extract them from other non-lane features. The entire method was illustrated using detailed examples and the effectiveness of the proposed method was tested on real road traffic data collected on highways and major roads. It was seen that the proposed method detects lane markings with high accuracy during day time and late evenings. It is proposed to extend this research to night videos also as future work.

References

[1] Z. Kim, "Robust lane detection and tracking in challenging scenarios," in *IEEE Transactions on Intelligent Transportation Systems*, vol. 9, no. 1, March 2008, pp. 16 – 26.

[2] J. McCall and M. Trivedi, "Video-based lane estimation and tracking for driver assistance: Survey, system and evaluation," in *IEEE Transactions on Intelligent Transportation Systems*, vol. 7, no. 1, March 2006, pp. 20 – 37.

[3] P. Lindner, S. Blokzyl, G. Wanielik, and U. Scheunert, "Applying multi level processing for robust geometric lane feature extraction," in *Multisensor Fusion and Integration for Intelligent Systems (MFI), 2010 IEEE Conference on*, Sept. 2010, pp. 248 –254.

[4] F. Coskun, O. Tuncer, M. Karsligil, and L. Guvenc, "Real time lane detection and tracking system evaluated in a hardware-in-the-loop simulator," in *Intelligent Transportation Systems (ITSC), 2010 13th International IEEE Conference on*, Sept. 2010, pp. 1336 –1343.

[5] S. Zhou, Y. Jiang, J. Xi, J. Gong, G. Xiong, and H. Chen, "A novel lane detection based on geometrical model and gabor filter," in *Intelligent Vehicles Symposium (IV), 2010 IEEE*, June 2010, pp. 59 –64.

[6] J. Lee, C. Kee, and U. Yi, "A new approach for lane departure identification," in *Intelligent Vehicles Symposium, 2003. Proceedings. IEEE*, June 2003, pp. 100 – 105.

[7] L.-W. Tsai, J.-W. Hsieh, C.-H. Chuang, and K.-C. Fan, "Lane detection using directional random walks," in *Intelligent Vehicles Symposium, 2008 IEEE*, June 2008, pp. 303 –306.

[8] Y. Otsuka, S. Muramatsu, H. Takenaga, Y. Kobayashi, and T. Monj, "Multitype lane markers recognition using local edge direction," in *Intelligent Vehicle Symposium, 2002. IEEE*, vol. 2, June 2002, pp. 604 – 609 vol.2.

[9] R. C. Gonzalez and R. E. Woods, *Digital Image Processing*, 2nd ed. Prentice Hall, 2002.

[10] R. Satzoda, S. Suchitra, and T. Srikanthan, "Gradient angle histograms for efficient linear hough transform," in *Image Processing (ICIP), 2009 16th IEEE International Conference on*, Nov. 2009, pp. 3273 –3276.